chemengineering

MDPI

Article

Enhanced Removal of Chlorpyrifos, Cu(II), Pb(II), and Iodine from Aqueous Solutions Using Ficus Nitida and Date Palm Biochars

Essam R. I. Mahmoud [1,*], Hesham M. Aly [2], Noura A. Hassan [3], Abdulrahman Aljabri [1], Asim Laeeq Khan [4] and Hashem F. El-Labban [5]

[1] Department of Mechanical Engineering, Faculty of Engineering, Islamic University of Madinah, Madinah 42351, Saudi Arabia; aaljabri@iu.edu.sa
[2] Department of Forestry and Timber Trees, Horticulture Research Institute, Agricultural Research Center, Antoniadis Botanical Garden, Alexandria 21554, Egypt; hesham.aly@arc.sci.eg
[3] Pesticide Chemistry & Technology Department, Faculty of Agriculture, Alexandria University, Alexandria 21545, Egypt; noura.hassan@alexu.edu.eg
[4] Department of Chemical Engineering, Faculty of Engineering, Islamic University of Madinah, Madinah 42351, Saudi Arabia; akhan@iu.edu.sa
[5] Production Engineering Department, Faculty of Engineering, Alexandria University, El-Chatby, Alexandria 21544, Egypt; dr_labbanh@alexu.edu.eg
* Correspondence: emahoud@iu.edu.sa

Abstract: This study explores the adsorption efficiency of biochar derived from palm trees and Ficus nitida for the removal of various contaminants, including Cu(II), Pb(II), iodine, and chlorpyrifos from aqueous solutions. Biochar was prepared using a two-step pyrolysis process for date palm biochar and single-step pyrolysis for Ficus nitida biochar. Characterization techniques such as SEM, EDX, and FTIR revealed a significant surface area and a variety of functional groups in both types of biochar, essential for effective adsorption. The date palm biochar exhibited superior adsorption capacities for Cu(II) and Pb(II) ions, achieving efficiencies up to 99.9% and 100%, respectively, due to its high content of oxygen-containing functional groups that facilitated strong complexation and ion exchange mechanisms. Conversely, Ficus nitida biochar demonstrated a higher adsorption capacity for iodine, reaching 68% adsorption compared to 39.7% for date palm biochar, owing to its greater surface area and microporosity. In the case of chlorpyrifos, Ficus nitida biochar again outperformed date palm biochar, achieving a maximum adsorption efficiency of 87% after 24 h of incubation, compared to 50.8% for date palm biochar. The study also examines the effect of incubation time on adsorption efficiency, showing that the adsorption of chlorpyrifos by date palm biochar increased significantly with time, reaching a maximum of 62.9% after 48 h, with no further improvement beyond 12 h. These results highlight the importance of biochar characteristics, such as surface area, pore structure, and functional groups, in determining adsorption efficiency. The findings suggest that optimizing pyrolysis conditions and surface modifications could further enhance the performance of biochar as a cost-effective and sustainable solution for water purification and environmental remediation.

Keywords: biochar; adsorption; heavy metals; chlorpyrifos; water purification

Citation: Mahmoud, E.R.I.; Aly, H.M.; Hassan, N.A.; Aljabri, A.; Khan, A.L.; F. El-Labban, H. Enhanced Removal of Chlorpyrifos, Cu(II), Pb(II), and Iodine from Aqueous Solutions Using Ficus Nitida and Date Palm Biochars. *ChemEngineering* **2024**, *8*, 105. https://doi.org/10.3390/chemengineering8050105

Academic Editor: Timothy Hunter

Received: 7 August 2024
Revised: 28 September 2024
Accepted: 8 October 2024
Published: 12 October 2024

1. Introduction

Heavy metal contamination resulting from industrial waste, natural processes, or anthropogenic activities can be considered as one of the most significant environmental issues for water resources [1–3]. Most of the heavy metals found in wastewater are considered toxic and carcinogenic to humans [2]. Previous studies have reported that effluent from several industries contains heavy metals (Cu, Pb, Cr, Fe, and Zn) with concentrations far above the standards set by the WHO [4].

Copper and lead are considered two of the most harmful elements due to their extensive use and their negative impact. Industrial processes such as machining, forging, rolling,

extrusion, and the use of copper-based fungicides in agriculture are primary contributors to the release of copper, particularly in its toxic soluble form, Cu(II), into water bodies [5]. Some operations such as refining processes, automobile maintenance, and batteries produce a large amount of toxic lead (Pb) which has harmful effects on water quality, the environment, and human health [6,7]. Iodine, which originates from the food, chemical, and pharmaceutical industries, and nuclear power plants, can also cause environmental contamination [8–11]. It is very harmful due to its high toxicity to the thyroid glands, and the occurrence of hypothyroidism in cases of excessive amounts [12,13]. In addition to heavy metals, environmental contamination from industrial processes introduces pesticide residues like chlorpyrifos into water bodies. These pollutants pose significant health risks, such as genotoxicity, endocrine disruption, and neurological issues, necessitating efficient and cost-effective removal technologies.

To address the issue of contaminant removal from wastewater, various techniques have been introduced by researchers. These include membrane filtration, oxidation, chemical precipitation, microbial degradation, ion exchange, solvent extraction, coagulation, electrocoagulation, steam stripping, and adsorption [14,15]. However, many of these methods are resource-intensive and require substantial electrical power. Among these methods, adsorption stands out due to its ease of implementation, flexibility, multiple benefits, high renewability, and cost-effectiveness, particularly in terms of regeneration for reuse. Carbon-based adsorbents, such as biochar, are especially effective for the adsorption of toxic metals like Cu(II) and Pb(II), as well as other pollutants, including iodine and chlorpyrifos, from contaminated water [16,17].

Biochar, which is considered as one of the natural and simple carbon-based adsorbents, can be used for metal removal from aqueous solutions. This biochar can be derived from agricultural waste or biomass through a low-temperature pyrolysis process [18]. Campos et al. [3] prepared biochar from rice husks, olive pits, and wood chips and used it to absorb Cu(II) and Pb(II) from aqueous solution [3]. In another study, Ghanim [19] produced high-quality biochar from date pits [19]. Recently, Alghamdi and Alasmary [20] prepared biochar from date palm waste and magnetized it through Fe-intercalation, and used it to adsorb Cd(II) and Pb(II) ions from wastewater [20]. The adsorption capacity of the magnetic biochar is higher than that of normal biochar. Another study has been undertaken to remove Pb(II) and Cd(II) from synthetic waste solutions using palm fibers chemically treated with sulfuric acid, oxalic acid, HNO_3, and Na_2SO_3 [21]. The palm fibers treated with sulfuric acid gave the highest adsorption percentages. Mahdi et al. [22] described in detail the preparation of biochar from date seed biomass and used it for lead ion (Pb(II)) adsorption from an aqueous solution, and it was found that the best adsorption conditions are pyrolysis at a temperature of 550 °C for a holding time of 3 h and a pH of nearly 6. Al-Fulaiti et al. [23] reported that the best performance in the adsorption of iodine from aqueous solutions is using cyclodextrin (CD) derivatives (α, β, γ and β-hydroxypropyl-CD) [24]. Cyclodextrin is a non-toxic, biodegradable material, and it is a cyclic oligosaccharide macromolecule [24,25]. I_2 molecules can be adsorbed on the hydrophobic chains and in CD hydrophobic cavities [26]. As described by Windiastuti et al. [27], iodine can also be adsorbed from an aqueous solution through low-cost biochar, prepared from empty oil palm bunches by the application of a hydrothermal carbonation process [27]. The biochar was activated before and after pyrolysis by heating it using an autoclave at 121 °C for 90 min. In these treatments, alkaline activators were used. Biochar was then soaked using NaOH or KOH with a concentration of 0%, 4%, 8%, and 12% for 3 h. The results showed that the adsorption of iodine ranged from 208.86–616.32 mg/g [27].

In this study, we explore biochar derived from Ficus nitida and date palm waste—two abundant and underutilized resources in Saudi Arabia. These biochar materials exhibit unique structural and chemical properties that enhance their adsorption efficiency. The biochar produced in this study is expected to have a high surface area, porosity, and a diverse range of functional groups, making it highly effective for the adsorption of Cu(II), Pb(II), iodine, and chlorpyrifos pesticide from contaminated water. By utilizing locally

available waste materials, this research not only addresses the critical environmental issue of water contamination but also promotes sustainable waste management practices. The findings provide valuable insights for developing cost-effective and efficient adsorbents, contributing to the broader goal of ensuring clean and safe water resources through sustainable technologies.

2. Materials and Methods

2.1. Biochar Preparation

In this study, biochar was prepared from the mid-ribs of date palm leaves collected from Al-Madinah Al-Munawara, Saudi Arabia. The preparation process involved a slow pyrolysis technique executed in two distinct steps using a vacuum furnace. Initially, the samples were air-dried for four weeks to remove moisture content. Subsequently, the dried specimens were heated at a controlled rate of 10 °C per minute up to 300 °C. This temperature was maintained for a holding time of 1 h to facilitate the partial decomposition of organic materials. The samples were then allowed to cool overnight to room temperature to stabilize the intermediate products. In the second step, the specimens were reheated at the same controlled rate of 10 °C per minute, but this time up to a higher temperature of 600 °C. The holding time at this temperature was also 1 h. This step was crucial for further decomposing the organic materials and enhancing the carbonization process, resulting in a biochar with a high surface area and increased porosity. After this second heating phase, the samples were once again cooled overnight to room temperature. The two-step pyrolysis process ensures the production of biochar with desirable structural and functional properties, suitable for adsorption applications.

For the preparation of biochar from Ficus nitida, branches were collected and subjected to an initial air-drying process for about three weeks. This drying period was essential to reduce the moisture content and facilitate the subsequent pyrolysis process. After drying, the branches were debarked and sawn into suitable pieces to maximize surface area and ensure uniform pyrolysis. The prepared samples were then subjected to pyrolysis under oxygen-limited conditions in a muffle furnace. The absence of oxygen is critical to prevent combustion and ensure proper carbonization of the biomass. The furnace temperature was raised to 500 °C and maintained for a holding time of 60 min. This temperature and duration were selected based on the thermal decomposition characteristics of Ficus nitida, aiming to maximize the development of micropores and functional groups on the biochar surface. Following the pyrolysis, the biochar was allowed to cool to room temperature. The cooled biochar was then ground to a fine powder to increase the surface area and enhance its adsorption capabilities. Finally, the ground biochar was stored in sealed bags to prevent contamination and maintain its quality for subsequent use. Figures 1 and 2 summarize the preparation procedures for date palm and Ficus nitida biochar, respectively.

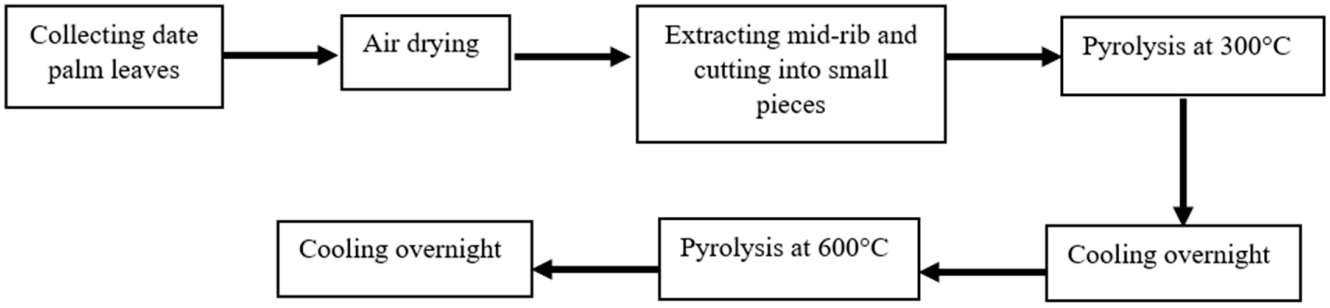

Figure 1. Schematic illustration for preparation steps of date palm biochar.

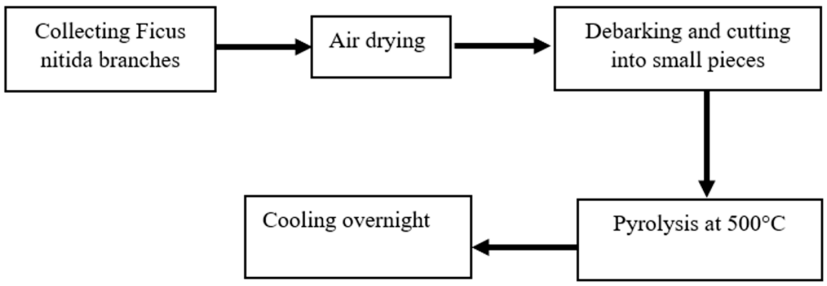

Figure 2. Schematic illustration for preparation steps of Ficus nitida biochar.

2.2. Biochar Characterization

For the characterization of both types of biochar, a comprehensive approach was taken to understand their structural and chemical properties. The microstructures of the biochar surfaces were meticulously investigated using a scanning electron microscope (Jeol JSM-5300 SEM, Tokyo, Japan) equipped with an energy-dispersive X-ray (EDX) analyzer. SEM was utilized to capture high-resolution images of the biochar surface morphology, revealing details about the porosity, texture, and structural features. EDX analysis complemented the SEM imaging by providing elemental composition data, identifying the types and quantities of elements present on the biochar surfaces. This dual analysis enabled a thorough examination of the physical and elemental characteristics of the biochar, which are crucial for understanding its adsorption properties. To identify the functional groups present on the biochar surface, Fourier transform infrared (FTIR) spectroscopy was employed. The analysis was performed using a Burker Tensor 37 spectrometer (Karlsruhe, Germany), operating in the spectral range of 400–4000 cm^{-1}. The FTIR technique involves measuring the absorption of infrared radiation by the biochar sample, which provides information about the various functional groups attached to the biochar surface. The KBr pellet technique was used to prepare the biochar samples for FT-IR analysis. Specifically, 1.0 mg of finely ground biochar was intimately mixed with 100 mg of potassium bromide (KBr). The mixture was then compressed into a transparent pellet under high pressure. This pellet was subsequently placed in the path of an infrared beam in the spectrometer. The resulting FT-IR spectra displayed peaks corresponding to different functional groups, such as hydroxyl, carbonyl, and aromatic groups, which play a vital role in the adsorption processes. The comprehensive characterization of the biochar using SEM, EDX, and FTIR provided detailed insights into surface morphology, elemental composition, and functional group distribution. These characteristics are essential for evaluating and optimizing the biochar's effectiveness in adsorbing heavy metals and pesticides from aqueous solutions.

2.3. Adsorption of Heavy Metals by Biochar

The adsorption of Cu(II), Pb(II), and iodine from aqueous media was investigated using biochar prepared from date palm and Ficus nitida. For all pollutants, stock solutions were prepared, and biochar concentrations were varied to assess adsorption efficiency. For the adsorption of Cu(II) and Pb(II), stock solutions of 1000 ppm $CuSO_4 \cdot 5H_2O$ and 100 ppm Pb(II) were prepared, respectively. Different concentrations of biochar (20, 40, 60, and 80 mg) were incubated with 10 mL of 200 ppm Cu(II) or 100 ppm Pb(II) solutions for 24 h. The remaining concentrations of Cu(II) and Pb(II) were determined using atomic absorption spectroscopy (ContrAA 300, Jena, Germany) after filtration with a 0.2 µm syringe filter. For iodine, a 0.1 M stock solution was prepared, and biochar samples were incubated with 50 mL of the iodine solution for 1 h. The residual iodine concentration was determined by titration using Na_2SO_3 0.1 N in the presence of a starch indicator. Adsorption efficiency was monitored over time, with incubation periods ranging from 2 to 30 h.

The percentage of adsorption (%Ads) was calculated as follows:

$$\%\text{Ads} = \frac{\textit{Conc. in control} - \textit{conc. in treatment}}{\textit{conc. in control}} \times 100$$

2.4. Adsorption of Chlorpyrifos by Biochar

A solution of 1000 ppm of chlorpyrifos, with a chemical structure shown in Figure 3, was prepared in acetone with the presence of tween 80 as an emulsifier then diluted with distilled water to a final concentration of 100 ppm. About 10 mL of the chlorpyrifos solution was incubated with different amounts of biochar for 24 h then filtered with a syringe filter of 0.2 µm, and the residual concentration was determined using HPLC. A constant amount of biochar was incubated with 10 mL of chlorpyrifos solution 100 ppm for interval times of 3, 6, 12, 24, and 48 h. Then, the solution was filtered and determined using HPLC.

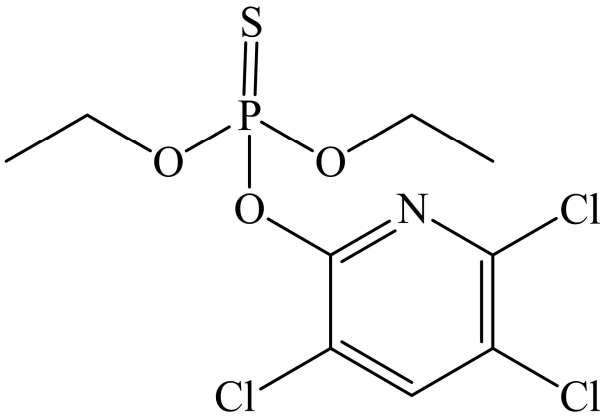

Figure 3. Chemical structure of chlorpyrifos.

Chlorpyrifos residues were performed on high-performance liquid chromatography (Agilent 1260 HPLC Infinity system, Waldbronn, Germany) equipped with a variable wavelength ultraviolet detector (VWD). The system consists of a quaternary gradient pump to control the flow rate of the mobile phase, an autosampler for automatic injection, a vacuum degasser, and a column thermostat (5–80 °C). Five microliters of each sample were injected onto the reversed-phase ZORBAX Eclipse Plus C18 column (250° 4.6 mm id, 5 mm particle size) using the autosampler apparatus with a 100 µL sample loop. Data were managed using HP Chem station software (B.04.03). The mobile phase was acetonitrile: water (40:60, *v/v*) and the flow rate was 1 mL/min and the temperature of the column was 40 °C. The detector wavelengths (nm) were 242 and 233 for acetamiprid and methomyl, respectively. The retention times of acetamiprid and methomyl were 3.96 ± 0.04 and 2.795 ± 0.03 min, respectively.

3. Results and Discussion

3.1. Main Features and Functional Groups of Biochar Surfaces

Figure 1 illustrates the microstructures of biochar surfaces produced from date palm (Figure 4a) and Ficus nitida (Figure 4b). A large number of well-organized and relatively uniform enlarged pores are found in both types of biochar. The large and uniform pores are obtained due to more efficient evaporation of volatiles and other organic components resulting from the application of the two-step pyrolysis process with the applied conditions. Such pores aid in the improvement of the biochar's adsorption properties, particularly in the removal of pollutants [28].

Figure 5 illustrates the EDX analysis for the two types of biochar. These results indicate that carbon and oxygen are the most abundant elements in both types. However, the percentage of carbon is higher than that of oxygen. The high temperature of pyrolysis (600 °C) facilitates the dehydration and volatilization processes, resulting in an increased carbon content [29]. Traces of other elements such as magnesium, sodium, silicon, phosphorus, and sulfur are only observed in the date palm biochar, while calcium and potassium are observed in the two types of biochar, as listed in Table 1. The presence of elements like

magnesium and silicon at high pyrolysis temperatures can be attributed to the insoluble metallic oxides found in the biochar samples [28,29].

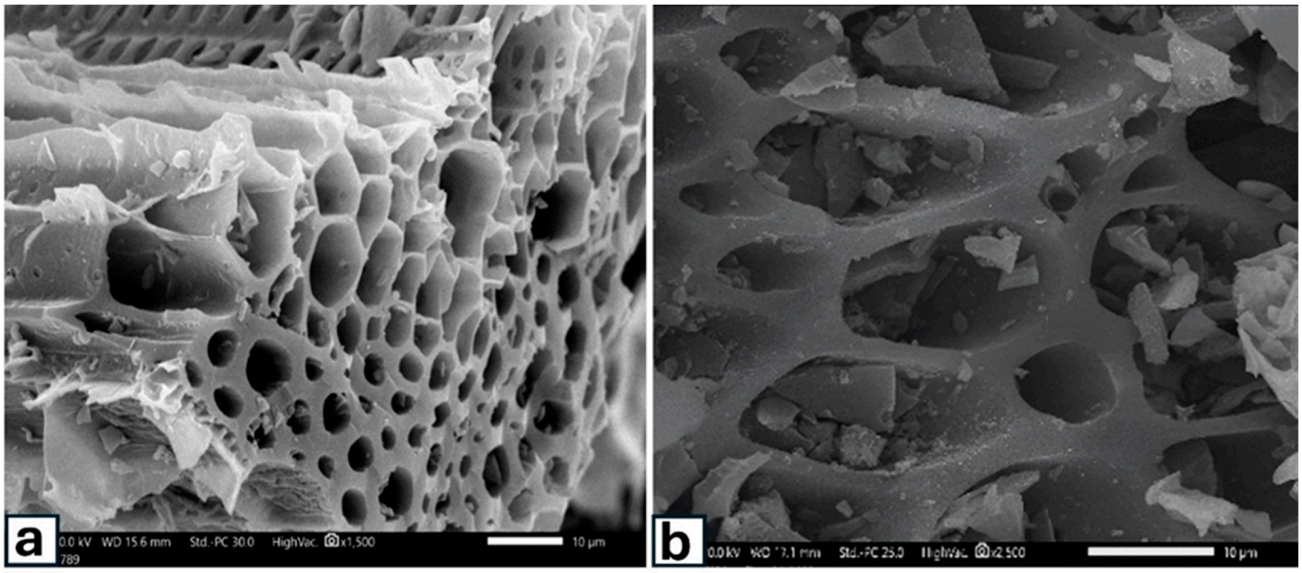

Figure 4. SEM images for the microstructures of surfaces of the two types of biochar: (**a**) date palm biochar and (**b**) Ficus nitida biochar.

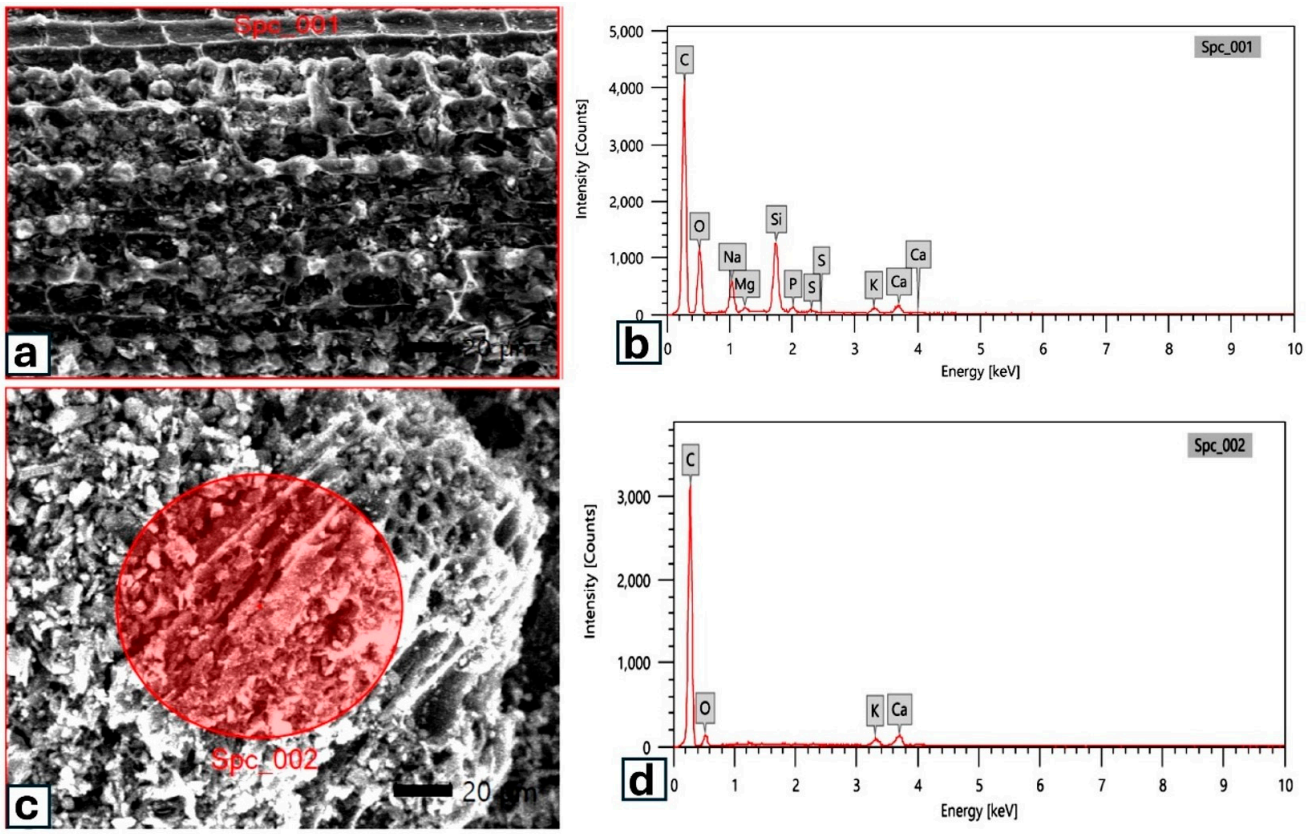

Figure 5. Electron dispersive X-ray (EDX) images of biochar prepared from date palm (**a**,**b**) and Ficus nitida (**c**,**d**).

FTIR spectra for the two types of biochar prepared from date palm and Ficus nitida are shown in Figures 6a and 6b, respectively, and the results of these spectra are summarized in Table 2. The bands recorded between 3200 to 3700 cm^{-1} and observed in both types of

biochar confirm the presence of stretching vibration of the O-H group. It is typically associated with the hydrogen-bonded O-H group in carboxylic and phenolic compounds [30,31]. Aliphatic substitution of aromatic rings can be confirmed by the presence of methyl groups observed for two types at 2088–3000 cm^{-1} [31]. The presence of ring stretching C=C was confirmed in both biochars by the peak noticed around 1560 cm^{-1} [32]. Peaks recorded between 1600 and 1800 cm^{-1} in the Ficus nitida biochar may confirm the vibration of C=C in aromatics or may attributed to C=O for carboxyl or carbonate lactones [33]. Bands recorded in both types at 1420 cm^{-1} correspond to aliphatic C-H groups [30]. The peaks that were also recorded in the range of 1000–1240 cm^{-1} for both types are assigned to the stretching C-O group in phenolic, alcoholic compounds and carboxylic acids [34], also at the range of 1000–1100 cm^{-1}, can be attributed to asymmetric Si-O stretching [35] and may be confirmed by the results of EDX in which a traces of silicon were observed for the date palm biochar. All bands observed for both biochars in the range of 400–600 cm^{-1} are assigned to organic matter such as carbonate and silicates [36]. In addition, bands in the 700–900 cm^{-1} range, associated with C-H out-of-plane bending in substituted aromatic rings, further confirm the presence of aromatic structures [37,38] in both types of biochar. The physicochemical properties of biochar are mainly affected by the biomass material, and the conditions of pyrolysis (heating rate, temperature, and holding time) [34]. The pores and surface functional groups, particularly carbonyl, hydroxyl, and methyl, represent the main features of the surface which affect its adsorption efficiency [39,40]. In addition, other oxygen-rich functional groups on the biochar surface, such as carboxyl and phenolic hydroxyl groups, play a crucial role in the adsorption of heavy metals [41].

Table 1. Elemental analysis of both types of biochar as observed by electron dispersive X-ray.

Element	Biochar Type	
	Date palm	Ficus nitida
	Mass % ± SD	Mass % ± SD
C	62.06 ± 0.21	72.93 ± 0.39
O	27.89 ± 0.31	23.80 ± 0.71
Mg	0.28 ± 0.02	--
Na	3.32 ± 0.07	--
Si	4.37 ± 0.06	--
P	0.46 ± 0.02	--
S	0.17 ± 0.01	--
Ca	0.54 ± 0.03	1.11 ± 0.09
K	0.91 ± 0.03	2.16 ± 0.11
O/C ratio	0.45	0.33

FTIR analysis of the biochar before and after the adsorption (Figure 6c,d) of chlorpyrifos reveals distinct changes in functional groups, confirming their involvement in the adsorption process. For Ficus nitida biochar, the disappearance of bands corresponding to the -OH group suggests that these groups actively participated in the interaction with chlorpyrifos. This interaction is further supported by the notable shifts in the carbonyl (C=O) and C-O bond intensities, which are indicative of complexation and interaction with oxygen-containing functional groups during adsorption. Similarly, in the case of date palm biochar, the reduction in intensity of the C=C bands after adsorption points towards π–π interactions with the aromatic ring of chlorpyrifos. The shift in the C-O bond, along with changes in the hydroxyl group bands, demonstrates that these functional groups facilitated the adsorption process, most likely through hydrogen bonding and electrostatic interactions. The differences in the FTIR spectra before and after adsorption highlight the critical role of these surface functional groups in enhancing the adsorption efficiency of chlorpyrifos on both types of biochar [42].

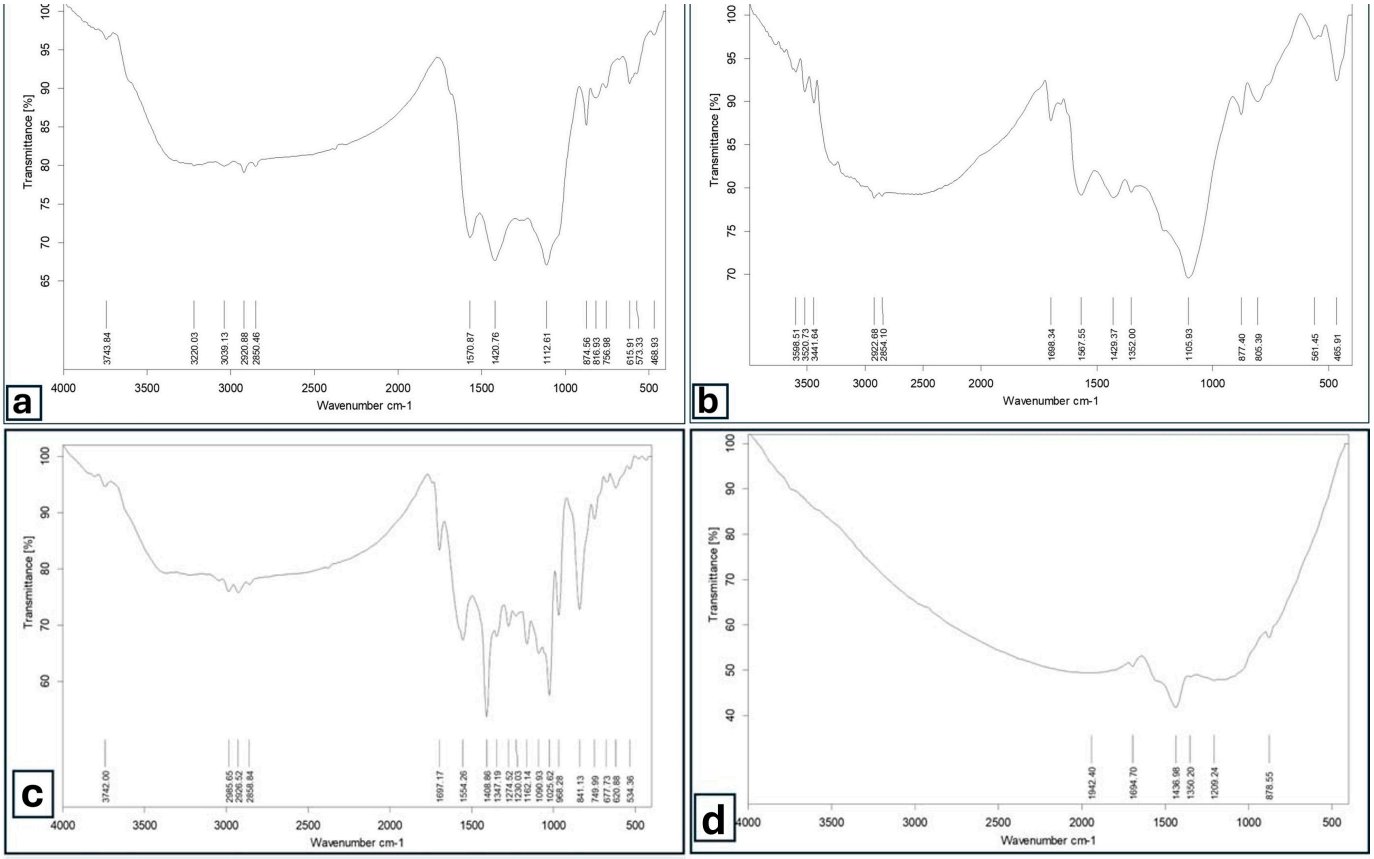

Figure 6. FTIR spectra of biochar prepared from date palm before adsorption (**a**), Ficus nitida before adsorption (**b**), date palm after adsorption (**c**), and Ficus nitida after adsorption (**d**).

Table 2. FTIR bands and corresponding functional groups.

Wave Number (cm^{-1})	Assignments
3000–3700	-OH group
2800–3000	C-H (methyl)
≈2000	C-C
1600–1800	C=O/COOH
1560	C=C
1420–1450	C-H asymmetric
1317–1375	C-O asymmetric of aromatic
1000–1260	C-O
700–900	C-H aromatic (out of plan)
400–600	In organic matter

3.2. Adsorption of Cu(II) from Aqueous Solution on Different Amounts of Biochar

The adsorption of Cu(II) ions from aqueous solutions was evaluated using biochar prepared through a two-step pyrolysis process, resulting in a material with a highly porous structure and elevated carbon content. This porous structure enhances the biochar's capacity to attract and retain copper ions through electrostatic interactions. The specific pyrolysis conditions employed not only maximized the porosity but also led to the formation of functional groups observed in the biochar, such as hydroxyl, carbonyl, and phenolic groups. The ion exchange mechanism also plays a critical role in the adsorption process. The negatively charged sites on the biochar surface interact with the positively charged copper cations (Cu(II)), enabling effective ion exchange and subsequent removal of copper ions from the solution.

The efficiency of the biochar in adsorbing copper ions was quantitatively assessed by measuring the absorbance of Cu(II) at different concentrations, as depicted in Table 3 and Figure S1. The data demonstrate a strong linear relationship between Cu(II) concentration and absorbance, confirming the high adsorption capacity of the biochar. Remarkably, the date palm biochar achieved adsorption efficiencies ranging from 99.11% to 99.9% with the addition of small amounts, proving its effectiveness. These findings validate the superior performance of date palm-derived biochar in removing Cu(II) from aqueous solutions, attributable to its optimized structural properties and functional group composition. The results highlight the potential of using this biochar as a cost-effective and sustainable adsorbent for heavy metal remediation in water treatment applications.

Table 3. Adsorption of Cu(II) (200 ppm) on different amounts of biochar.

Amount of Biochar (g/10 mL)	Ficus nitida Biochar		Date palm Biochar	
	The Mean Concentration of Cu(II) (mg/L)	% of Adsorption	The Mean Concentration of Cu(II) (mg/L)	% of Adsorption
0.02	125.6	37	42	79
0.04	56.8	72	1.78	99.11
0.06	35	83	0.6	99.7
0.08	23.8	88	0.2	99.9

As shown in Table 3, the efficiency of date palm biochar in the removal of Cu(II) from the aqueous solution, in all cases of addition, is higher than that of Ficus nitida biochar. Elemental analysis revealed that the percentage of oxygen in date palm biochar is higher compared to Ficus nitida biochar, leading to an increase in oxygen-based functional groups. These groups significantly enhance the biochar's adsorption efficiency for Cu(II). Similar results have been observed by other researchers, where biochar produced from hardwood and corn stalks showed maximum copper ion removal percentages of up to 95%, while biochar from rice husks, compost, and orange waste exhibited lower efficiencies [43,44]. The date palm leaf midrib biochar, therefore, optimizes its structural properties and enhances the presence of functional groups, making it more effective for copper adsorption. Consequently, this transformation of date palm waste into useful biochar offers an ecological solution for water purification and heavy metal remediation.

3.3. Adsorption of Pb(II) from Aqueous Solution on Different Amounts of Biochar

As stated in the case of Cu(II)adsorption, different amounts of biochar (0.02, 0.04, 0.06, and 0.08 g/10 mL) were added to absorb Pb(II) from the aqueous solution. The linear relationship between different concentrations of Pb(II) and the corresponding absorbance in the case of date palm biochar is illustrated in Table 4. The data indicate that increasing the amount of biochar enhances the adsorption percentage of Pb(II). Table 4 lists the mean concentration of Pb(II) (mg/L) and its adsorption (%) for both date palm and Ficus nitida biochar.

Table 4. Adsorption of Pb(II) on different amounts of both types of biochar.

Amount of Biochar (g/10 mL)	Date palm Biochar		Ficus nitida Biochar	
	The Mean Concentration of Pb(II) (mg/L)	% of Adsorption	The Mean Concentration of Pb(II) (mg/L)	% of Adsorption
0.02	0.15	99.9	24.6	75
0.04	0.11	99.9	19. 4	80
0.06	0	100	15.1	85
0.08	0	100	8.1	92

The results show that with the addition of a small amount (0.02 g/10 mL) of date palm biochar, 99.85% adsorption of Pb(II) from the aqueous solution was achieved. In comparison, the same amount of Ficus nitida biochar resulted in a lower adsorption percentage of 75.38%. When the amount of date palm biochar was increased to 0.06 or 0.08 g/10 mL, 100% adsorption of Pb(II) was observed. However, for the same amounts of Ficus nitida biochar, the adsorption percentages were 84.96% and 91.87%, respectively. These findings highlight the superior biosorption efficiency of date palm biochar in removing Pb(II) from aqueous solutions.

Several mechanisms contribute to the removal of Pb(II), including precipitation, complexation, ion exchange, electrostatic attraction, and physical adsorption [45]. The precipitation mechanism was confirmed by detecting Pb(II) particles on the biochar surface, attributed to the precipitation of carbonate minerals and phosphates [46,47]. The efficiency of mineral precipitation is further enhanced with increased pyrolysis temperature. The presence of C-O groups combined with a significant amount of Pb in solution indicates surface complexation. Generally, the complexation ability of hydroxyl groups is more effective than that of carboxyl groups [48]. Ion exchange occurs between the cations on oxygen-containing functional groups and Pb ions [49], while Pb can also combine with -COOH and -OH groups on the biochar surface through electrostatic interactions [50].

Various removal mechanisms, such as precipitation, complexation, ion exchange, electrostatic attraction, chemical bond adsorption, and physical adsorption, play significant roles in Pb+2 removal [45]. The detection of Pb particles on the biochar surface due to the precipitation of carbonate minerals and phosphates confirms that precipitation is one of the main Pb removal mechanisms [46–52]. The precipitation of Pb ions is pH-dependent, with local high alkalinity sites on the biochar surface forming at pH > 6.0, leading to precipitation [53,54]. Higher pyrolysis temperatures enhance the effect of mineral precipitation [47]. Complexation, involving the interaction of electrons with donors and acceptors, is crucial for Pb adsorption by biochar, although its significance decreases at higher pyrolysis temperatures [47]. During the adsorption process, surface complexation occurs, with C-O groups binding a large amount of Pb [55,56]. The metal complexing ability of hydroxyl groups surpasses that of carboxyl groups [48]. Ion exchange between cations on oxygen-containing functional groups and Pb ions, along with electrostatic interactions involving -COOH and -OH groups, also contribute to Pb removal [49,50].

The retention of toxic metals by various forest tree species has been extensively reviewed [57]. Ficus nitida, in particular, has been utilized by several investigators for the adsorption of Pb, Cu, and Cd [58]. In one study, biochar prepared from $KMnO_4$-treated hickory wood through slow pyrolysis at 600 °C demonstrated increased surface oxygen-containing functional groups, resulting in strong sorption abilities for Pb(II), Cu(II), and Cd(II) [59]. Various researchers have described the strong bonding affinity of oxygen-containing functional groups, such as hydroxyl, phenolic hydroxyl, and carboxyl groups, to heavy metal ions in aqueous solutions [43].

3.4. Adsorption of Iodine on Different Amounts of Biochar

To investigate the effects of biochar type and dosage on the removal of iodine from aqueous solutions, different amounts of biochar (0.1, 0.2, 0.3, and 0.4 g/50 mL) were added to iodine solutions. The adsorption efficiency was evaluated by measuring the residual iodine concentration in each case. The results, detailed in Table 5, reveal significant differences in iodine adsorption between Ficus nitida and date palm biochar. For the highest biochar dosage of 0.4 g/50 mL, Ficus nitida biochar exhibited an adsorption efficiency of 68%, while date palm biochar achieved a lower adsorption efficiency of 39.7%. These differences can be attributed to the inherent structural and chemical properties of the two biochar types. Ficus nitida biochar, with its higher surface area and greater pore volume, provides more active sites for iodine adsorption. The increased presence of functional groups, such as hydroxyl (-OH) and carboxyl (-COOH) groups, on the Ficus nitida biochar surface enhances its ability to form interactions with iodine molecules. These functional

groups facilitate both physisorption and chemisorption processes, leading to higher iodine uptake. In contrast, date palm biochar, despite having a considerable adsorption capacity, has a lower surface area and fewer active sites compared to Ficus nitida biochar. The lower efficiency of date palm biochar in iodine adsorption can be attributed to its structural limitations and the lesser availability of functional groups essential for iodine interaction. The observed adsorption trends underscore the importance of biochar characteristics in determining their effectiveness for specific contaminant removal. The higher efficiency of Ficus nitida biochar highlights its potential as a superior adsorbent for iodine removal in water treatment applications. Further optimization of pyrolysis conditions and surface modifications could enhance the adsorption capabilities of both biochar types, providing cost-effective and sustainable solutions for water purification.

Table 5. Adsorption of iodine on different amounts of both types of biochar.

Amount of Biochar (g/50 mL)	Biochar Type	
	Date palm	Ficus nitida
	% of Adsorption	% of Adsorption
0.1	24	18
0.2	27	31
0.3	33	46.8
0.4	39	68

The effect of incubation time on the adsorption efficiency of iodine by date palm biochar was studied by incubating 0.4 g of biochar with an iodine solution for varying periods, ranging from 2 to 30 h. As illustrated in Figure 7, the adsorption percentage increased with the incubation time, reaching a maximum of 60.3% after 12 h. Beyond this incubation period, up to 30 h, no further significant increase in adsorption was observed, and the maximum adsorption remained at 60.3%. The initial increase in adsorption efficiency can be attributed to the biochar's surface functional groups and its microstructural properties. The biochar's surface area and the presence of micropores play a crucial role in enhancing its iodine adsorption capacity. As the incubation period increases, more iodine molecules diffuse into the biochar's micropores, which are less than 2 nm in size, and interact with the functional groups present on the biochar surface [60–62]. The adsorption indices for iodine are generally related to the availability and distribution of these micropores [63]. Despite the high adsorption capacity observed, the percentages of iodine adsorption are lower than those of Pb(II) on date palm biochar. This discrepancy is primarily due to the larger pore size distribution in date palm biochar, which may not be as effective in adsorbing smaller iodine molecules compared to larger Pb(II) ions. Activated carbon, on the other hand, undergoes high-temperature activation processes that create a more extensive network of smaller pores, thereby exhibiting higher iodine adsorption capacities [64,65]. Additionally, the presence of surface impurities on biochar can react chemically with iodine, affecting its iodine number—a parameter that indicates the capacity for iodine adsorption [66,67]. High levels of oxygen-containing functional groups, such as carboxyl groups, can reduce the iodine number due to their reactivity with potassium iodide [68]. This interaction can lead to a decrease in the effective adsorption capacity of the biochar for iodine. These findings highlight the critical role of biochar's structural and chemical properties in determining its adsorption efficiency for different contaminants. Optimizing the pyrolysis conditions and possibly introducing surface modifications could enhance the iodine adsorption capacity of date palm biochar, making it a more versatile adsorbent for water purification applications.

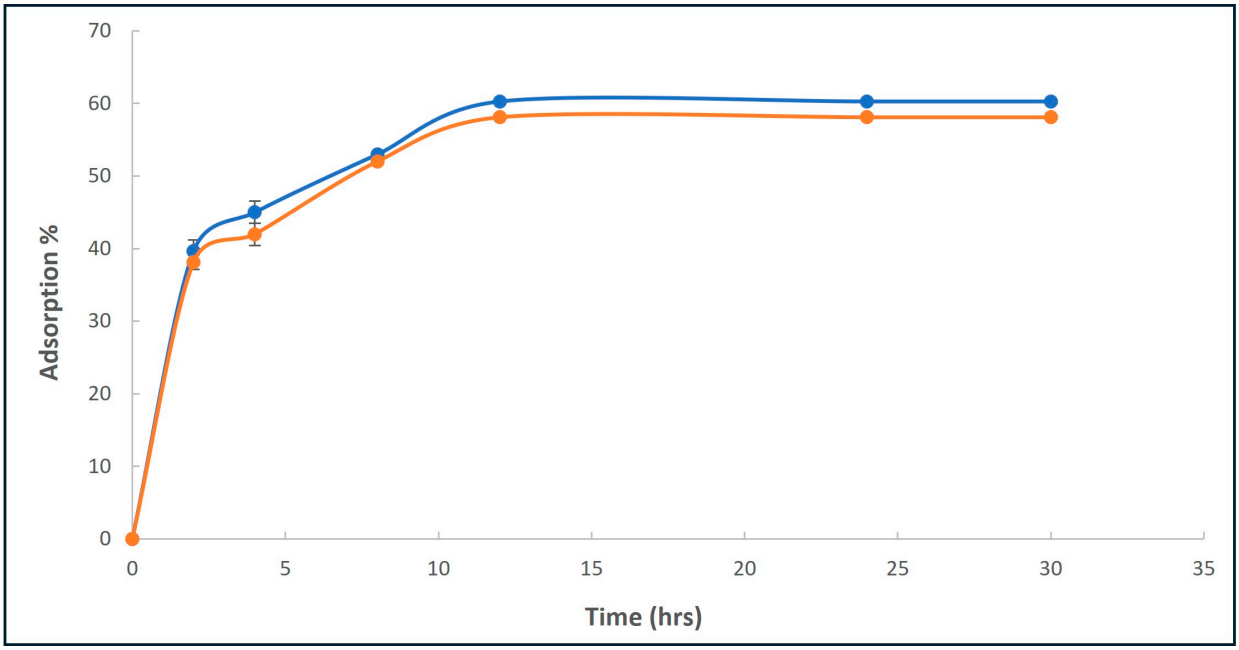

Figure 7. Adsorption of iodine on date palm biochar (——) and Ficus nitida biochar (——) after different incubation times.

3.5. Adsorption of Chlorpyrifos on Biochar

The adsorption of chlorpyrifos on different amounts of biochar was systematically investigated, and the results are presented in Table 6. The data reveal a significantly higher adsorption capacity of Ficus nitida biochar compared to date palm biochar. Specifically, after an incubation period of 24 h, the adsorption efficiency for a maximum biochar amount of 0.08 g/10 mL was 87% for Ficus nitida biochar, whereas date palm biochar exhibited a lower adsorption efficiency of 50.8%. The superior performance of Ficus nitida biochar can be attributed to its inherent structural and chemical properties. The biochar derived from Ficus nitida has a higher surface area and a greater number of adsorption sites compared to date palm biochar. These characteristics are crucial for enhancing the interaction between the biochar surface and chlorpyrifos molecules, thereby facilitating higher adsorption efficiencies. The adsorption process is largely driven by the presence of functional groups, such as hydroxyl (-OH) and carboxyl (-COOH) groups, which are more prevalent on the surface of Ficus nitida biochar. These functional groups play a vital role in binding chlorpyrifos molecules through various mechanisms, including hydrogen bonding, π–π interactions, and Van der Waals forces. The trend of increasing adsorption percentages with the amount of biochar is consistent with the availability of more adsorption sites as the biochar dosage increases [69]. This increase in adsorption sites enhances the probability of chlorpyrifos molecules interacting with the biochar surface, thus improving the overall adsorption efficiency. Additionally, the porous nature of the biochar, especially in the case of Ficus nitida, provides ample space for the chlorpyrifos molecules to be trapped and retained within the pore structures. It is also important to consider the specific surface chemistry of the biochar. The Ficus nitida biochar, due to its higher content of oxygen-containing functional groups, exhibits stronger interactions with chlorpyrifos molecules. These functional groups can form stable complexes with chlorpyrifos, thus enhancing its adsorption capacity. On the other hand, date palm biochar, while still effective, has fewer active sites and functional groups, resulting in lower adsorption efficiencies.

For the addition of 0.08 g/10 mL of date palm biochar, the adsorption percentages of chlorpyrifos were evaluated after different incubation periods of 3, 6, 12, 24, and 48 h. The results, illustrated in Figure 8, demonstrate that increasing the incubation period from 3 to 12 h leads to a significant increase in adsorption efficiency, from approximately 37% to 60%.

Beyond 12 h, no substantial improvement in adsorption was observed, with the maximum adsorption percentage reaching 62.9% at 48 h. The initial increase in adsorption efficiency can be attributed to the availability of surface functional groups and the porous structure of the biochar. The biochar's ability to adsorb chlorpyrifos is significantly influenced by its surface area and the presence of micropores. As the incubation period increases, more chlorpyrifos molecules are able to diffuse into these micropores and interact with the functional groups present on the biochar surface. These interactions include hydrogen bonding, Van der Waals forces, and π–π interactions, which facilitate the retention of chlorpyrifos molecules within the biochar matrix.

Table 6. Percentage of adsorption of chlorpyrifos (100 ppm) on different amounts of both types of biochar.

Amount of Biochar (g/10 mL)	Biochar Type	
	Date palm % of Adsorption	Ficus nitida % of Adsorption
0.02	14	18
0.04	26	50
0.06	29	62
0.08	50	87

The study conducted by various investigators [70–72] evaluated the efficiency of conventional water treatment methods, rice husk biochar, commercial activated carbon, and Ficus nitida biochar for the removal of chlorpyrifos from water. Their results indicated that rice husk biochar is particularly efficient for chlorpyrifos removal, suggesting its potential as a cost-effective alternative to commercial activated carbon [70]. Further studies demonstrated that biochar prepared from rice straw at high temperatures (300 °C, 400 °C, 500 °C, and 600 °C) could adsorb multiple herbicides simultaneously, enhancing the degradation of these herbicides in soil. In another study, biochar derived from Ficus nitida tree residues was prepared at 500 °C and 700 °C. This biochar, both alone and as a carrier for frankincense essential oil, showed significant insecticidal activity against stored product insects such as *Tribolium castaneum*, *Rhyzopertha dominica*, and *Oryzaephilus surinamensis*. The biochar prepared at 500 °C was particularly effective, with *O. surinamensis* being the most susceptible [71]. These findings highlight the versatile applications of Ficus nitida biochar in both environmental and agricultural contexts. In the present study, FTIR analysis revealed the presence of numerous functional groups on the surface of Ficus nitida biochar, including carboxyl (-COOH) and hydroxyl (-OH) groups. These functional groups enhance the biochar's adsorption capacity by providing active sites for chlorpyrifos binding [72–74]. Additionally, the adsorption process is influenced by the intraparticle diffusion of chlorpyrifos molecules into the micropores of the biochar, which affects the diffusion rate to the exterior surface of the adsorbent [75]. Due to its non-toxic nature, biochar can be safely utilized for environmental remediation and recycling purposes. The intraparticle diffusion mechanism plays a crucial role in the adsorption process, as it governs the rate at which micro-pollutants penetrate the micropores and interact with the internal surface area of the biochar [75]. These findings emphasize the potential of using date palm biochar for the adsorption of chlorpyrifos and other pollutants, underscoring the importance of optimizing biochar properties to enhance its adsorption efficiency for various environmental applications.

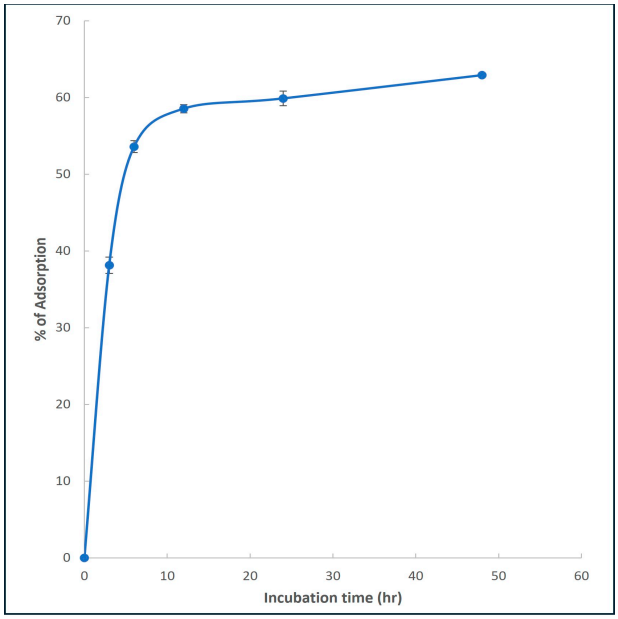

Figure 8. Adsorption of chlorpyrifos on date palm biochar after different incubation times. Error bars describe the standard deviation of three replicates.

3.6. Regeneration of Biochar for Cu(II) Adsorption

The regeneration potential of an adsorbent is a critical parameter for determining its sustainability and reusability in multiple adsorption cycles. To evaluate the regeneration capability of date palm biochar, a study was conducted using 0.08 g of biochar per 10 mL of Cu(II) solution, where the initial adsorption efficiency reached 99.9%. The biochar was subjected to five consecutive adsorption–desorption cycles, as shown in Figure 9. The results indicate that the biochar retained high adsorption efficiency throughout the cycles, with a marginal reduction in performance by the fifth cycle.

The adsorption efficiency during each cycle remained above 96%, demonstrating excellent regeneration potential. This slight reduction in adsorption over multiple cycles could be attributed to partial pore saturation or minor structural changes in the biochar surface during the regeneration process. However, the overall performance remained robust, highlighting the biochar's suitability for long-term applications in water treatment, especially for removing Cu(II) ions.

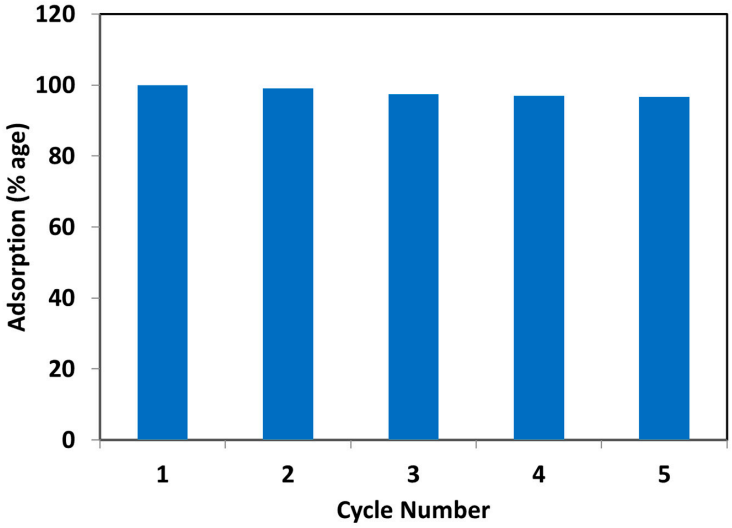

Figure 9. Effect of repeated cycles on the adsorption capacity of date palm biochar.

4. Conclusions

This study investigated the adsorption efficiency of biochar derived from palm trees and Ficus nitida for the removal of various contaminants, including Cu(II), Pb(II), iodine, and chlorpyrifos from aqueous solutions. The biochar was prepared using a two-step pyrolysis process for date palm biochar and single-step pyrolysis for Ficus nitida biochar. Characterization techniques, including SEM, EDX, and FTIR, revealed that both types of biochar possess a significant surface area and a variety of functional groups essential for effective adsorption. The date palm biochar demonstrated a higher adsorption capacity for Cu(II) ions compared to Ficus nitida biochar, with adsorption efficiencies ranging from 99.11% to 99.9%. This higher capacity is attributed to the high percentage of oxygen-containing functional groups on the date palm biochar surface, which facilitated strong complexation and ion exchange mechanisms. Similarly, the date palm biochar also showed superior performance in removing Pb(II) ions from aqueous solutions, achieving up to 100% adsorption at higher biochar dosages. The primary mechanisms involved included precipitation, complexation, ion exchange, and electrostatic interactions.

In contrast, the Ficus nitida biochar exhibited a higher adsorption capacity for iodine, achieving 68% adsorption at the highest dosage, compared to 39.7% for date palm biochar. This increased efficiency is due to the greater surface area and functional groups present in Ficus nitida biochar. The study also highlighted the importance of micropores in determining iodine adsorption capacities. Furthermore, Ficus nitida biochar outperformed date palm biochar in the adsorption of chlorpyrifos, with a maximum adsorption efficiency of 87% after 24 h of incubation, compared to 50.8% for date palm biochar. The higher adsorption capacity of Ficus nitida biochar for chlorpyrifos can be attributed to its structural characteristics and the presence of functional groups that enhance interaction with chlorpyrifos molecules.

The effect of incubation time on the adsorption efficiency was also examined, showing that the adsorption percentage increased significantly with incubation time, reaching a maximum of 62.9% for chlorpyrifos on date palm biochar after 48 h. The initial rapid increase in adsorption was due to the availability of adsorption sites, with no significant improvement observed beyond 12 h of incubation. These findings underscore the importance of biochar characteristics, such as surface area, pore structure, and functional groups, in determining adsorption efficiency. Optimizing pyrolysis conditions and surface modifications could further enhance the performance of biochar as a cost-effective and sustainable solution for water purification and environmental remediation.

Supplementary Materials: The following supporting information can be downloaded at: https://www.mdpi.com/article/10.3390/chemengineering8050105/s1, Figure S1: The relationship between the concentrations of Cu (II) and the corresponding absorbance in the case of palm tree biochar; Figure S2: The relationship between the concentrations of Pb (II) and the corresponding absorbance in the case of palm tree biochar.

Author Contributions: Conceptualization, E.R.I.M. and H.M.A.; methodology, H.M.A. and H.F.E.-L.; validation, E.R.I.M., H.M.A. and N.A.H.; formal analysis, H.M.A.; investigation, N.A.H.; resources, N.A.H.; data curation, H.F.E.-L.; writing—review and editing, H.F.E.-L. and A.L.K.; visualization, H.M.A. and A.A.; supervision, A.L.K.; project administration, A.A.; funding acquisition, E.R.I.M. All authors have read and agreed to the published version of the manuscript.

Funding: This research received no external funding.

Data Availability Statement: The data will be available on request.

Acknowledgments: The authors would like to express their appreciation for the support provided by the Scientific Research Deanship, Islamic University of Madinah. During the preparation of this work, the authors used ChatGPT to refine writing and improve readability. The authors have reviewed and edited the AI-generated content as necessary and take full responsibility for the contents of this publication.

Conflicts of Interest: The authors declare no conflicts of interest.

References

1. Manikandan, S.; Subbaiya, R.; Saravanan, M.; Ponraj, M.; Selvam, M.; Pugazhendhi, A. A critical review of advanced nanotechnology and hybrid membrane-based water recycling, reuse, and wastewater treatment processes. *Chemosphere* **2022**, *289*, 132867. [CrossRef] [PubMed]
2. Mansoor, S.; Kour, N.; Manhas, S.; Zahid, S.; Wani, O.A.; Sharma, V.; Wijaya, L.; Alyemeni, M.N.; Alsahli, A.A.; El-Serehy, H.A. Biochar as a tool for effective management of drought and heavy metal toxicity. *Chemosphere* **2021**, *271*, 129458. [CrossRef] [PubMed]
3. Campos, P.; De la Rosa, J.M. Assessing the Effects of Biochar on the Immobilization of Trace Elements and Plant Development in a Naturally Contaminated Soil. *Sustainability* **2020**, *12*, 6025. [CrossRef]
4. Lewoyehu, M. Comprehensive review on synthesis and application of activated carbon from agricultural residues for the remediation of venomous pollutants in wastewater. *J. Anal. Appl. Pyrolysis* **2021**, *159*, 105279. [CrossRef]
5. Abd Elnabi, M.K.; Elkaliny, N.E.; Elyazied, M.M.; Azab, S.H.; Elkhalifa, S.A.; Elmasry, S.; Mouhamed, M.S.; Shalamesh, E.M.; Alhorieny, N.A.; Abd Elaty, A.E.; et al. Toxicity of Heavy Metals and Recent Advances in Their Removal: A Review. *Toxics* **2023**, *11*, 580. [CrossRef]
6. Hashem, A.; Fletcher, A.; Younis, H.; Mauof, H.; Abou-Okeil, A. Adsorption of Pb (II) ions from contaminated water by 1,2,3,4-butanetetracarboxylic acid-modified microcrystalline cellulose: Isotherms, kinetics, and thermodynamic studies. *Int. J. Biol. Macromol.* **2020**, *164*, 3193–3203. [CrossRef]
7. Dai, K.; Liu, G.; Xu, W.; Deng, Z.; Wu, Y.; Zhao, C.; Zhang, Z. Judicious fabrication of bifunctionalized graphene oxide/MnFe2O4 magnetic nanohybrids for enhanced removal of Pb (II) from water. *J. Colloid Interface Sci.* **2020**, *579*, 815–822. [CrossRef]
8. Abidli, A.; Huang, Y.; Rejeb, Z.B.; Zaoui, A.; Park, C.B. Sustainable and efficient technologies for removal and recovery of toxic and valuable metals from wastewater: Recent progress, challenges, and future perspectives. *Chemosphere* **2022**, *292*, 133102. [CrossRef]
9. Hikmat Hama Aziz, K.H.; Kareem, R. Recent advances in water remediation from toxic heavy metals using biochar as a green and efficient adsorbent: A review. *Case Stud. Chem. Environ. Eng.* **2023**, *8*, 100495. [CrossRef]
10. Abdelmoaty, Y.H.; Tessema, T.D.; Choudhury, F.A.; El-Kadri, O.M.; El-Kaderi, H.M. Nitrogen rich porous polymers for carbon dioxide and iodine sequestration for environmental remediation. *ACS Appl. Mater. Interfaces* **2018**, *10*, 16049. [CrossRef]
11. Zhang, T.; Yue, X.; Gao, L.; Qiu, F.; Xu, J.; Rong, J.; Pan, J. Hierarchically porous bismuth oxide/layered double hydroxide composites: Preparation, characterization, and iodine adsorption. *J. Clean. Prod.* **2017**, *144*, 220. [CrossRef]
12. Luo, Y.; Kawashima, A.; Ishido, Y.; Yoshihara, A.; Oda, K.; Hiroi, N.; Ito, T.; Ishii, N.; Suzuki, K. Iodine excess as an environmental risk factor for autoimmune thyroid disease. *Int. J. Mol. Sci.* **2014**, *15*, 12895. [CrossRef] [PubMed]
13. Nallapaneni, A.; Pope, C.N. Chlorpyrifos. In *Encyclopedia of Toxicology*, 2nd ed.; Wexler, P., Ed.; Elsevier: Amsterdam, The Netherlands, 2005; pp. 583–585.
14. Huang, L.; Wu, B.; Wu, Y.; Yang, Z.; Yuan, T.; Alhassan, S.I.; Yang, W.; Wang, H.; Zhang, L. Porous and flexible membrane derived from ZIF-8-decorated hyphae for outstanding adsorption of Pb^{2+} ion. *J. Colloid Interface Sci.* **2020**, *565*, 465–473. [CrossRef]
15. Shen, M.; Song, B.; Zeng, G.; Zhang, Y.; Teng, F.; Zhou, C. Surfactant changes lead adsorption behaviors and mechanisms on microplastics. *Chem. Eng. J.* **2020**, *405*, 126989. [CrossRef]
16. Mahmoud, E.R.I.; Aly, H.M.; Hassan, N.A.; Abdulrahman Aljabri, A.; Khan, A.L.; El-Labban, H.F. Biochar from Date Palm Waste via Two-Step Pyrolysis: A Modified Approach for Cu (II) Removal from Aqueous Solutions. *Processes* **2024**, *12*, 1189. [CrossRef]
17. Akhil, D.; Lakshmi, D.; Kartik, A.; Vo, D.V.N.; Arun, J.; Gopinath, K.P. Production, characterization, activation, and environmental applications of engineered biochar: A review. *Environ. Chem. Lett.* **2021**, *19*, 2261–2297. [CrossRef]
18. Rani, L.; Kaushal, J.; Lal Srivastav, A. Biochar as sustainable adsorbents for chromium ion removal from aqueous environment: A review. *Biomass Convers. Bioref.* **2024**, *14*, 6083–6096. [CrossRef]
19. Ghanim, A.N. Utilization of date pits derived bio-adsorbent for heavy metals in wastewater treatment: Review. *Al-Qadisiyah J. Eng. Sci.* **2023**, *16*, 058–069. [CrossRef]
20. Alghamdi, A.G.; Alasmary, Z. Efficient Remediation of Cadmium- and Lead-Contaminated Water by Using Fe-Modified Date Palm Waste Biochar-Based Adsorbents. *Int. J. Environ. Res. Public Health* **2023**, *20*, 802. [CrossRef]
21. Thabeta, W.M.; Ahmedb, S.B.; Abdelwahaba, O.; Soliman, N.F. Enhancement Adsorption of Lead and Cadmium Ions from Waste Solutions Using Chemically Modified Palm fibers. *Egypt. J. Chem.* **2020**, *63*, 14917–14927. [CrossRef]
22. Mahdi, Z.; Yu, Q.J.; El Hanandeh, A. Removal of lead(II) from aqueous solution using date seed-derived biochar: Batch and column studies. *Appl. Water Sci.* **2018**, *8*, 181. [CrossRef]
23. Al-Fulaiti, B.; El-Shafey, E.S.I.; Al Kindi, S.H.S.; Abdel-Jalil, R.J. Adsorption of Iodine from Aqueous Solution on Modified Silica Gel with Cyclodextrin Derivatives. *Pol. J. Environ. Stud.* **2022**, *31*, 5571–5582. [CrossRef] [PubMed]
24. Barman, B.K.; Barman, S.; Roy, M.N. Inclusion complexation between tetrabutylphosphonium methanesulfonate as guest and α- and β-cyclodextrin as hosts investigated by physicochemical methodology. *J. Mol. Liq.* **2018**, *264*, 80. [CrossRef]
25. Mahmoud, E.R.I.; Aly, H.M.; Hassan, N.A.; Abdulrahman Aljabri, A.; Khan, A.L.; El-Labban, H.F. Utilizing Date Palm Leaf Biochar for Simultaneous Adsorption of Pb(II) and Iodine from Aqueous Solutions. *Processes* **2024**, *12*, 1370. [CrossRef]
26. Hirota, M.; Higaki, S.; Ito, S.; Ishida, Y.; Terao, K. Effects of 2-hydroxypropyl α-cyclodextrin on the radioactive iodine sorption on activated carbon. *J. Radioanal. Nucl. Chem.* **2021**, *328*, 659. [CrossRef]

27. Windiastuti, E.; Indrasti, N.S.; Hasanudin, U.; Suprihatin, Y.B. The Influence of Pretreatment and Post Treatment with Alkaline Activators on the Adsorption Ability of Biochar from Palm Oil Empty Fruit. *J. Ecol. Eng.* **2023**, *24*, 242–251. [CrossRef]
28. Usman, A.R.A.; Abduljabbar, A.; Vithanage, M.; Ok, Y.S.; Ahmad, M.; Ahmad, M.; Elfaki, J.; Abdulazeem, S.S.; Al-Wabel, M.I. Biochar production from date palm waste: Charring temperature induced changes in composition and surface chemistry. *J. Anal. Appl. Pyrol.* **2015**, *115*, 392–400. [CrossRef]
29. Wang, Y.; Zhu, Y.; Cheng, Y.; Jiang, P. Online analysis method for pyrolysis products with large volatility difference at high temperature and pressure: Pyrolysis kinetics of supercritical pressure n-decane. *Fuel* **2023**, *346*, 128245. [CrossRef]
30. Cantrell, K.B.; Hunt, P.G.; Uchimiya, M.; Novak, J.M.; Ro, K.S. Impact of pyrolysis temperature and manure source on physicochemical characteristics of biochar. *Bioresour. Technol.* **2012**, *107*, 419–428. [CrossRef]
31. Pasieczna-Patkowska, S.; Madej, J. Comparison of photoacoustic, diffuse reflectance attenuated total reflectance and transmission infrared spectroscopy for the study of biochar. *Pol. J. Chem. Technol.* **2018**, *20*, 75–83. [CrossRef]
32. Abdulrazzaq, H.; Jol, H.; Husni, A.; Abu-Bakr, R. Characterization and stabilisation of biochars obtained from empty fruit bunch, wood, and rice husk. *BioResources* **2014**, *9*, 2888–2898. [CrossRef]
33. Alcazar-Ruiz, A.; Dorado, F.; Sanchez-Silva, L. Bio-phenolic compounds production through fast pyrolysis: Demineralizing olive pomace pretreatments. *Food Bioprod. Process.* **2023**, *137*, 200–213. [CrossRef]
34. Yu, J.; Sun, J.; Sun, M.; Li, W.; Qi, D.; Zhang, Y.; Han, C. Protective mechanism of Coprinus comatus polysaccharide on acute alcoholic liver injury in mice, the metabolomics and gut microbiota investigation. *Food Sci. Hum. Wellness* **2024**, *13*, 401–413. [CrossRef]
35. Cavaglia, J.; Garcia, S.M.; Roger, J.M.; Mestres, M.; Boqué, R. Detection of bacterial spoilage during wine alcoholic fermentation using ATR-MIR and MCR-ALS. *Food Control* **2022**, *142*, 109269. [CrossRef]
36. Xue, T.; Wang, R.-Q.; Zhang, M.M.; Dai, J.-L. Adsorption, and desorption of mercury (II) in three forest soils in Shandong Province, China. *Pedosphere* **2013**, *23*, 265–272. [CrossRef]
37. Ye, Q.; Zhou, Y.; Xu, Y.; Zhang, Q.; Shi, X.; Li, D.; Tian, D.; Jiang, D. Improved charge transfer in polymeric carbon nitride synergistically induced by the aromatic rings modification and Schottky junctions for efficient photocatalytic CO_2 reduction. *Chem. Eng. J.* **2023**, *463*, 142395. [CrossRef]
38. Yan, J.; Li, Z.; Zhang, Y.; Liu, R.; Zhou, L.; Fu, P. Hydrodeoxygenation of lignin phenolic derivatives to aromatics: A review of catalyst functionalization for targeted deoxygenation and active site modification strategies. *Fuel Process. Technol.* **2023**, *250*, 107914. [CrossRef]
39. Ban, Y.; Jin, L.; Li, Y.; Yang, H.; Hu, H. Pyrolysis behaviors of model compounds with representative oxygen-containing functional groups in carbonaceous feedstock over calcium. *Fuel* **2023**, *335*, 127137. [CrossRef]
40. Sizirici, B.; Fseha, Y.H.; Yildiz, I.; Delclos, T.; Khaleel, A. The effect of pyrolysis temperature and feedstock on date palm waste derived biochar to remove single and multi-metals in aqueous solutions. *Sustain. Environ. Res.* **2021**, *31*, 9. [CrossRef]
41. Chen, H.; Xie, A.; You, S. A Review: Advances on Absorption of Heavy Metals in the Wastewater by Biochar. *IOP Conf. Ser. Mater. Sci. Eng.* **2018**, *301*, 012160. [CrossRef]
42. Tong, Y.; Mcnamara, P.J.; Mayer, B.K. Adsorption of organic micropollutants onto biochar: A review of relevant kinetics, mechanisms and equilibrium. *Environ. Sci. Water Res. Technol.* **2019**, *5*, 821–838. [CrossRef]
43. Chen, X.C.; Chen, G.C.; Chen, L.G.; Chen, Y.X.; Lehmann, J.; McBride, M.B.; Hay, A.G. Adsorption of copper and zinc by biochars produced from pyrolysis of hardwood and corn straw in aqueous solution. *Bioresour. Technol.* **2011**, *102*, 8877–8884. [CrossRef] [PubMed]
44. Goodman, B.A. Utilization of waste straw and husks from rice production: A review. *J. Bioresour. Bioprod.* **2020**, *5*, 143–162. [CrossRef]
45. Wang, C.; Wang, X.; Li, N.; Tao, J.; Yan, B.; Cui, X.; Chen, G. Adsorption of Lead from Aqueous Solution by Biochar: A Review. *Clean Technol.* **2022**, *4*, 629–652. [CrossRef]
46. Chang, J.; Zhang, H.; Cheng, H.; Yan, Y.; Chang, M.; Cao, Y.; Huang, F.; Zhang, G.; Yan, M. Spent Ganoderma lucidum substrate derived biochar as a new bio-adsorbent for Pb^{2+}/Cd^{2+} removal in water. *Chemosphere* **2020**, *241*, 125121. [CrossRef]
47. Yang, Z.; Hou, J.; Wu, J.; Miao, L. The effect of carbonization temperature on the capacity and mechanisms of Pb (II) adsorption by microalgae residue-derived biochar. *Ecotoxicol. Environ. Saf.* **2021**, *225*, 112750. [CrossRef]
48. Zhao, M.; Dai, Y.; Zhang, M.; Feng, C.; Qin, B.; Zhang, W.; Zhao, N.; Li, Y.; Ni, Z.; Xu, Z.; et al. Mechanisms of Pb and/or Zn adsorption by different biochars: Biochar characteristics, stability, and binding energies. *Sci. Total Environ.* **2020**, *717*, 136894. [CrossRef]
49. Yang, X.; Wan, Y.; Zheng, Y.; He, F.; Yu, Z.; Huang, J.; Wang, H.; Ok, Y.S.; Jiang, Y.; Gao, B. Surface functional groups of carbon-based adsorbents and their roles in the removal of heavy metals from aqueous solutions: A critical review. *Chem. Eng. J.* **2019**, *366*, 608–621. [CrossRef]
50. Zhao, T.; Yao, Y.; Li, D.; Wu, F.; Zhang, C.; Gao, B. Facile low-temperature one-step synthesis of pomelo peel biochar under air atmosphere and its adsorption behaviors for Ag (I) and Pb (II). *Sci. Total Environ.* **2018**, *640–641*, 73–79. [CrossRef]
51. Xu, Y.; Bai, T.; Li, Q.; Yang, H.; Yan, Y.; Sarkar, B.; Lam, S.S.; Bolan, N. Influence of pyrolysis temperature on the characteristics and lead (II) adsorption capacity of phosphorus-engineered poplar sawdust biochar. *J. Anal. Appl. Pyrolysis* **2020**, *154*, 105010. [CrossRef]

52. Fan, Y.; Wang, H.; Deng, L.; Wang, Y.; Kang, D.; Li, C.; Chen, H. Enhanced adsorption of Pb (II) by nitrogen and phosphorus co-doped biochar derived from Camellia oleifera shells. *Environ. Res.* **2020**, *191*, 110030. [CrossRef] [PubMed]
53. Mohan, D.; Singh, P.; Sarswat, A.; Steele, P.H.; Pittman, C.U., Jr. Lead sorptive removal using magnetic and nonmagnetic fast pyrolysis energy cane biochars. *J. Colloid Interface Sci.* **2015**, *448*, 238–250. [CrossRef] [PubMed]
54. Shi, J.; Fan, X.; Tsang, D.C.; Wang, F.; Shen, Z.; Hou, D.; Alessi, D.S. Removal of lead by rice husk biochars produced at different temperatures and implications for their environmental utilizations. *Chemosphere* **2019**, *235*, 825–831. [CrossRef]
55. Cheng, S.; Liu, Y.; Xing, B.; Qin, X.; Zhang, C.; Xia, H. Lead and cadmium clean removal from wastewater by sustainable biochar derived from poplar saw dust. *J. Clean. Prod.* **2021**, *314*, 128074. [CrossRef]
56. Gao, R.; Xiang, L.; Hu, H.; Fu, Q.; Zhu, J.; Liu, Y.; Huang, G. High-efficiency removal capacities and quantitative sorption mechanisms of Pb by oxidized rape straw biochars. *Sci. Total Environ.* **2019**, *699*, 134262. [CrossRef]
57. Balraju, W.; Upadhyay, K.K.; Tripathi, S.K. Remediation of Toxic Metals by Forest Trees: Concepts and Strategies. *Environ. Ecol.* **2022**, *40*, 1798–1810.
58. El-Khatib, A.A.; Barakat, N.A.; Youssef, N.A.; Samir, N.A. Bio accumulation of heavy metals air pollutants by urban trees. *Int. J. Phytoremed.* **2020**, *22*, 210–222. [CrossRef]
59. Wang, H.; Gao, B.; Wang, S.; Fang, J.; Xue, Y.; Yang, K. Removal of Pb(II), Cu(II), and Cd(II) from Aqueous Solutions by Biochar Derived from KMnO4 Treated Hickory Wood. 2015. Available online: http://www.elsevier.com/open-access/userlicense/1.0/ (accessed on 15 September 2024).
60. Yenisoy-Karakas, S.; Aygün, A.; Günes, M.; Tahtasakal, E. Physical and chemical characteristics of polymerbased spherical activated carbon and its ability to adsorb organics. *Carbon* **2004**, *42*, 477–484. [CrossRef]
61. Hernandez-Maglinao, J.; Capareda, S.C. Improving the Surface Areas and Pore Volumes of Biochar Produced from Pyrolysis of Cotton Gin Trash via Steam Activation Process. *Int. J. Eng. Sci.* **2019**, *3*, 15–18.
62. Saleh, M.E.; Mahmoud, A.H.; Rashad, M. Biochar usage as a cost-effective bio-sorbent for removing NH_4-N from wastewater. In Proceedings of the Global Climate Change, Biodiversity and Sustainability: An International Conference Focused on the Arab Mena Region and Euromed, Alexandria, Egypt, 15–19 April 2013; pp. 15–18.
63. Castiglioni, M.; Rivoira, L.; Ingrando, I.; Del Bubba, M.; Bruzzoniti, M.C. Characterization Techniques as Supporting Tools for the Interpretation of Biochar Adsorption Efficiency in Water Treatment: A Critical Review. *Molecules* **2021**, *26*, 5063. [CrossRef]
64. Jawad, A.H.; Abdulhameed, A.S.; Bahrudin, N.N.; Hum, N.N.M.F.; Surip, S.N.; Syed-Hassan, S.S.A.; Yousif, E.; Sabar, S. Microporous activated carbon developed from KOH activated biomass waste: Surface mechanistic study of methylene blue dye adsorption. *Water Sci. Technol.* **2021**, *84*, 1858–1872. [CrossRef] [PubMed]
65. Tamrin, K.F.; Zahrim, A.Y. Determination of optimum polymeric coagulant in palm oil mill effluent coagulation using multiple-objective optimisation on the basis of ratio analysis (MOORA). *Environ. Sci. Pollut. Res.* **2017**, *24*, 15863–15869. [CrossRef] [PubMed]
66. Schroder, A.; Kluppel, M.; Schuster, R.H.; Heidberg, J. Energetic surface heterogeneity of carbon black. *Kautsch. Gummi Kunststoffe.* **2001**, *54*, 260–266. Available online: http://www.plastverarbeiter.de/ai/resources/36a867629d7.pdf (accessed on 15 September 2024).
67. Wampler, W.A.; Nikiel, L.; Evans, E.N. Carbon black. In *Rubber Compounding: Chemistry and Applications*, 2nd ed.; Rodgers, B., Ed.; CRC Press: Boca Raton, FL, USA, 2016; Chapter 6; pp. 209–250.
68. Hess, W.M.; Herd, C.R. Microstructure, morphology, and general physical properties. In *Carbon Black: Science and Technology*, 2nd ed.; Donnet, J.-B., Bansal, R.C., Wang, M.J., Eds.; Marcel Dekker, Inc.: New York, NY, USA, 1993; Chapter 3; pp. 89–174.
69. Joshi, V.; Jindal, M.K.; Sar, S.K. Approaching a discussion on the detachment of chlorpyrifos in contaminated water using different leaves and peels as bio adsorbents. *Sci. Rep.* **2023**, *13*, 11186. [CrossRef]
70. Okoya, A.A.; Adegbaju, O.S.; Akinola, O.E.; Akinyele, A.B.; Amuda, O.S. Comparative Assessment of the Efficiency of Rice Husk Biochar and Conventional Water Treatment Method to Remove Chlorpyrifos from Pesticide Polluted Water. *CJAST* **2020**, *39*, CJAST.54205. [CrossRef]
71. Wahba, T.F.; Hassan, N.A.; Aly, H.M. Biochar prepared from Ficus nitida as a carrier for frankincense essential oil (*Boswellia sacra*) to control some stored product insects. *Pol. J. Entomol.* **2022**, *91*, 94–108. [CrossRef]
72. Liu, Y.; Yao, L.; Hu, B.; Li, T.; Tian, H. Adsorption Behavior and Residue Degradation of Triazine Herbicides in Soil Amended with Rice Straw Biochar. *Agriculture* **2023**, *13*, 1282. [CrossRef]
73. Klasson, K.T. Biochar characterization and a method for estimating biochar quality from proximate analysis results. *Biomass Bioenergy* **2017**, *96*, 50–58. [CrossRef]
74. Yaashikaa, P.R.; Kumar, P.S.; Sunita Varjani, S.; Saravanan, A. A critical review on the biochar production techniques, characterization, stability and applications for circular bioeconomy. *Biotechnol. Rep.* **2020**, *28*, 00570. [CrossRef]
75. Johnson, E. Utilization of Biochar Produced from Agricultural Residues for the Removal of Pesticide and Pharmaceutical Micropollutants in Surface Water Biofiltration. Ph.D. Thesis, School of Engineering, Newcastle University, Newcastle upon Tyne, UK, March 2022.